

# Nanostructures in Thermosetting Blends of Epoxy Resin with Polydimethylsiloxane-*block*-poly( $\epsilon$ -caprolactone)-*block*-polystyrene ABC Triblock Copolymer

Wenchun Fan, Lei Wang, and Sixun Zheng\*

Department of Polymer Science and Engineering and State Key Laboratory of Metal Matrix Composites, Shanghai Jiao Tong University, Shanghai 200240, P. R. China

Received August 7, 2008; Revised Manuscript Received November 9, 2008

**ABSTRACT:** Polydimethylsiloxane-*block*-poly( $\epsilon$ -caprolactone)-*block*-polystyrene ABC-type triblock copolymer (PDMS-*b*-PCL-*b*-PS) was synthesized via the sequential ring-opening polymerization and atom transfer radical polymerization. The ABC triblock copolymer was incorporated into epoxy to prepare the nanostructured thermosets. In terms of the difference in miscibility of epoxy with the subchains of the ABC triblock copolymer after and before curing reaction, it is proposed that the formation of the nanostructures follows the combined mechanisms of self-assembly and reaction-induced microphase separation. The self-organized nanophases could be formed before the curing reaction since the PDMS subchains of the triblock polymer is immiscible with the precursors of epoxy before curing reaction. The reaction-induced microphase separation of PS subchains occurred in the presence of the PDMS nanophases whereas the PCL subchains remain miscible with epoxy after and before curing reaction. By means of atomic force microscopy and small-angle X-ray scattering, the morphological structures of the thermosets containing the ABC triblock copolymer were examined, and the formation of the nanostructures was addressed on the basis of the combination of self-assembly and reaction-induced microphase separation mechanisms.

## Introduction

The formation of nanostructures in thermosets can optimize the interactions between thermosetting matrix and modifiers, and thus the properties of materials can be greatly improved.<sup>1,2</sup> Incorporating amphiphilic block copolymers into thermosets has been proved to be an efficient approach to access the ordered or disordered nanostructures in thermosets.<sup>3</sup> Hillmyer et al.<sup>3a,b</sup> first reported the strategy of creating the nanostructures via the mechanism of self-assembly. In this protocol, the precursors of thermosets act as the selective solvents of block copolymers; some self-organized nanophases such as lamellar, bicontinuous, cylindrical, and spherical structures can be created before the curing reaction depending on the concentration of block copolymers; these preformed nanophases were fixed via the subsequent curing reaction. More recently, it is identified that ordered and/or disordered nanostructures in thermosets can be alternatively formed via the mechanism of reaction-induced microphase separation (RIMS).<sup>4</sup> In this approach, it is not required that the amphiphilic block copolymers are self-organized into the nanophases before curing reaction; all the subchains of block copolymers may be miscible with precursors of thermosets. Upon curing, only a part of subchains of block copolymers are demixed to form the microphases.

A variety of block copolymer architectures have been employed to access ordered (or disordered) nanostructures in thermosets via self-assembly<sup>3</sup> or RIMS approaches.<sup>4</sup> In the previous work,<sup>3,4</sup> AB diblock and/or ABA triblock amphiphilic copolymers have been frequently employed to access the nanostructures of thermosets. However, few reports have been concerned with the formation of nanostructures in the thermosets containing ABC triblock copolymers.<sup>3i–k</sup> It is expected that the behavior of self-assembly or RIMS of ABC triblock copolymers in thermosets will be much more complicated than the cases of AB diblock or ABA triblock amphiphilic copolymers in thermosets. From the thermodynamic point of view, there are

three pairs of intercomponent interaction parameters between thermosetting matrix and the subchains of an ABC triblock copolymer, i.e.,  $\chi_{1A}$ ,  $\chi_{1B}$ , and  $\chi_{1C}$  (the subscripts 1, A, B, and C stand for thermosetting component, A, B, and C subchains of the block copolymer).<sup>5</sup> The simplest situation is that two blocks of the ABC triblock copolymer are miscible with the thermoset after and before curing reaction. In this case, the ABC triblock copolymer was transmuted into an amphiphile with respect of the thermoset. If two blocks of the ABC triblock copolymer are immiscible and one block is miscible with the thermoset, the competitive self-assembly (or RIMS) or RIMS in the presence of self-organized nanophases would be involved with the formation of its nanophases depending on the miscibility of the subchain with the thermosets after and before curing reaction, which provides tremendous space for maneuver to control the nanostructures of thermosets by tuning the interactions of blocks of ABC triblock copolymer with thermosets. However, such studies remain largely unexplored vis-à-vis the morphological control of thermosets using AB diblock or ABA triblock amphiphilic copolymers. It should be pointed out that Rebizant et al.<sup>3i–k</sup> have reported the formation of the ordered nanostructures in epoxy thermosets containing polystyrene-*block*-polybutadiene-*block*-poly(methyl methacrylate) ABC triblock copolymers (PS-*b*-PB-*b*-PMMA). In this system, the end block of the triblock copolymer (i.e., PMMA block) is miscible with epoxy after and before curing reaction, and the separated nanophases are composed of PS and PB subchains.

In this work, we synthesized a new ABC triblock copolymer, polydimethylsiloxane-*block*-poly( $\epsilon$ -caprolactone)-*block*-polystyrene (PDMS-*b*-PCL-*b*-PS); this block copolymer was incorporated into epoxy thermosets to obtain the nanostructured thermoset. The design of the ABC triblock copolymer is based on the following knowledge that (i) PDMS is immiscible with epoxy after and before curing reaction,<sup>3c,s,6</sup> (ii) PS undergoes reaction-induced phase separation in epoxy,<sup>4c,g–i</sup> and (iii) PCL is miscible with epoxy after and before curing reaction.<sup>6</sup> Therefore, both self-assembly and reaction-induced microphase separation mechanisms will concurrently be involved with the

\*To whom correspondence should be addressed: e-mail szheng@sjtu.edu.cn; Tel 86-21-54743278; Fax 86-21-54741297.

formation of the nanostructures in the thermosets. It is of interest to investigate the RIMS of PS subchain in the presence of PDMS nanophases. In this work, the nanostructures of the thermosets containing PDMS-*b*-PCL-*b*-PS triblock copolymer were investigated by means of atomic force microscopy and small-angle X-ray scattering. Differential scanning calorimetry was used to investigate the glass transition behavior of the nanostructures, and Fourier transform infrared spectroscopy was employed to examine the intermolecular hydrogen-bonding interactions between the miscible subchain and epoxy thermosets.

## Experimental Section

**Materials.** Diglycidyl ether of bisphenol A (DGEBA) with epoxide equivalent weight of 185–210 was purchased from Shanghai Resin Co., China. Monocarbonyl-terminated polydimethylsiloxane (PDMS-OH) was purchased from Gelest Co. under the trade name of MCR-C12, and it has a quoted molecular weight of  $M_n = 1400$  as well as  $M_w/M_n = 1.30$ . The curing agent is 4,4'-methylenebis(2-chloroaniline) (MOCA), supplied by Shanghai Reagent Co., China. Styrene is of analytically pure grade and was purchased from Shanghai Reagent Co., China. Prior to use, the inhibitor was removed by washing with aqueous NaOH (5 wt %) and deionized water for at least three times and dried by anhydrous  $MgSO_4$ ; the monomers were further distilled at reduced pressure.  $\epsilon$ -Caprolactone (99%) was purchased from Fluka Co., Germany, and it was dried over calcium hydride ( $CaH_2$ ) and distilled under decreased pressure. 2-Bromoisobutyl bromide and *N,N,N',N'*-pentamethyldiethylenetriamine (PMDETA) were purchased from Aldrich Co. and used as received. Copper(I) bromide (CuBr) was obtained from Shanghai Reagent Co., China, and it was purified according to the reported procedure.<sup>7</sup> Triethylamine was of analytically pure grade and was dried over  $CaH_2$  and then was refluxed with *p*-toluenesulfonyl chloride, followed by distillation. All other solvents used in this work are obtained from commercial resources and were purified according to standard procedures.

**Synthesis of PDMS-*b*-PCL Diblock Copolymer.** Monohydroxyl-terminated polydimethylsiloxane-*block*-poly( $\epsilon$ -caprolactone) diblock copolymer (PDMS-*b*-PCL-OH) was synthesized via ring-opening polymerization of  $\epsilon$ -caprolactone ( $\epsilon$ -CL) with the PDMS-OH as the initiator, and  $Sn(Oct)_2$  was used as the catalyst. Typically, PDMS-OH (3.50 g, 2.5 mmol) and  $\epsilon$ -CL (25.4 g, 222.8 mmol) were charged to a 100 mL round-bottom flask equipped with a dry magnetic stirring bar, and  $Sn(Oct)_2$  was added at the ratio of 2/1000 (w/w) with respect to CL using a syringe. The flask was connected to a standard Schlenk line, and the reactive mixture was degassed via three pump–freeze–thaw cycles and then immersed in a thermostated oil bath at 120 °C. The polymerization was carried out at 120 °C for 36 h to access the complete conversion of  $\epsilon$ -CL. The crude product was dissolved in tetrahydrofuran, and the solution was dropped into an excessive amount of petroleum ether to afford the precipitates; this procedure was repeated three times to obtain white solids. The product was dried in a vacuum oven until a constant weight was obtained with a yield of 93%. The molecular weight of the block copolymer was also determined by means of gel permeation chromatography to be  $M_n = 9300$  with  $M_w/M_n = 1.32$ .

**Synthesis of PDMS-*b*-PCL-*b*-PS Triblock Copolymer.** For the synthesis of PDMS-*b*-PCL-*b*-PS triblock copolymer, the PDMS-*b*-PCL-Br macroinitiator was first prepared by following the literature method.<sup>7</sup> The above PDMS-*b*-PCL-OH was used to react with 2-bromoisobutyl bromide in the presence of triethylamine to afford the 2-bromoisobutyl-terminated PDMS-*b*-PCL diblock copolymer (denoted PDMS-*b*-PCL-Br), which was further used as the macroinitiator of atom transfer radical polymerization for styrene to obtain the PDMS-*b*-PCL-*b*-PS triblock copolymer. To a 50 mL round-bottom flask, PDMS-*b*-PCL-Br macroinitiator (3.000 g, 0.400 mmol), CuBr (0.057 g, 0.400 mmol), PMDETA (83  $\mu$ L, 0.400 mmol), and styrene (7.819 g, 71 mmol) were charged. Connected to a standard Schlenk line system, the reactive system was degassed via three pump–freeze–thaw cycles and then immersed in a

thermostated oil bath at 110 °C. The polymerization was carried out for 8 h, and then the system was cooled to room temperature. The solvent THF was added to dissolve the product. After passing over a column of neutral alumina, the solution was concentrated and then dropped into an excessive amount of cold methanol to afford the precipitates. The PDMS-*b*-PCL-*b*-PS triblock copolymer was dried in vacuo at room temperature for 48 h. The polymer of 6.75 g was obtained with the conversion of styrene monomer being 48%. The molecular weight of PDMS-*b*-PCL-*b*-PS was measured by means of gel permeation chromatography to be  $M_n = 25\,600$  with  $M_w/M_n = 1.10$ . The triblock copolymer was also characterized by  $^1H$  NMR spectroscopy. The lengths of PDMS, PCL, and PS subchains in the triblock copolymer are  $M_n = 1400$ , 7900, and 16 300, respectively.

**Synthesis of Model PCL.** The model poly( $\epsilon$ -caprolactone) (PCL) was synthesized via the ring-opening polymerization (ROP) of  $\epsilon$ -CL with benzyl alcohol as the initiator, and  $Sn(Oct)_2$  was used as the catalyst. Typically, benzyl alcohol (0.3643 g, 3.37 mmol) and  $\epsilon$ -CL (27.7000 g, 240 mmol) were charged to a 100 mL round-bottom flask equipped with a dry magnetic stirring bar, and  $Sn(Oct)_2$  (1/1000 wt with respect to  $\epsilon$ -CL) was added using a syringe. The flask was connected to a standard Schlenk line, and the reactive mixture was degassed via three pump–freeze–thaw cycles and then immersed in a thermostated oil bath at 120 °C for 24 h. The crude product was dissolved in tetrahydrofuran, and the solution was dropped into an excessive amount of petroleum ether to afford the precipitates. This procedure was repeated three times to obtain white solids with the yield of 96%. The molecular weight of the PCL was estimated to be  $M_n = 7800$  according to the ratio of integration intensity of aliphatic methylene protons to aromatic protons in its  $^1H$  NMR spectrum.

**Preparation of Epoxy Thermosets.** The block copolymers (and/or the model PCL) were added to DGEBA at ambient temperature with continuous stirring until the homogeneous and transparent mixtures were obtained. After that, MOCA was added to systems with vigorous stirring until homogeneous blends were obtained. The ternary mixtures were poured into Teflon molds and cured at 150 °C for 2 h plus 180 °C for 2 h to access a complete curing reaction. The thermosetting blends containing block copolymers up to 40 wt % were prepared.

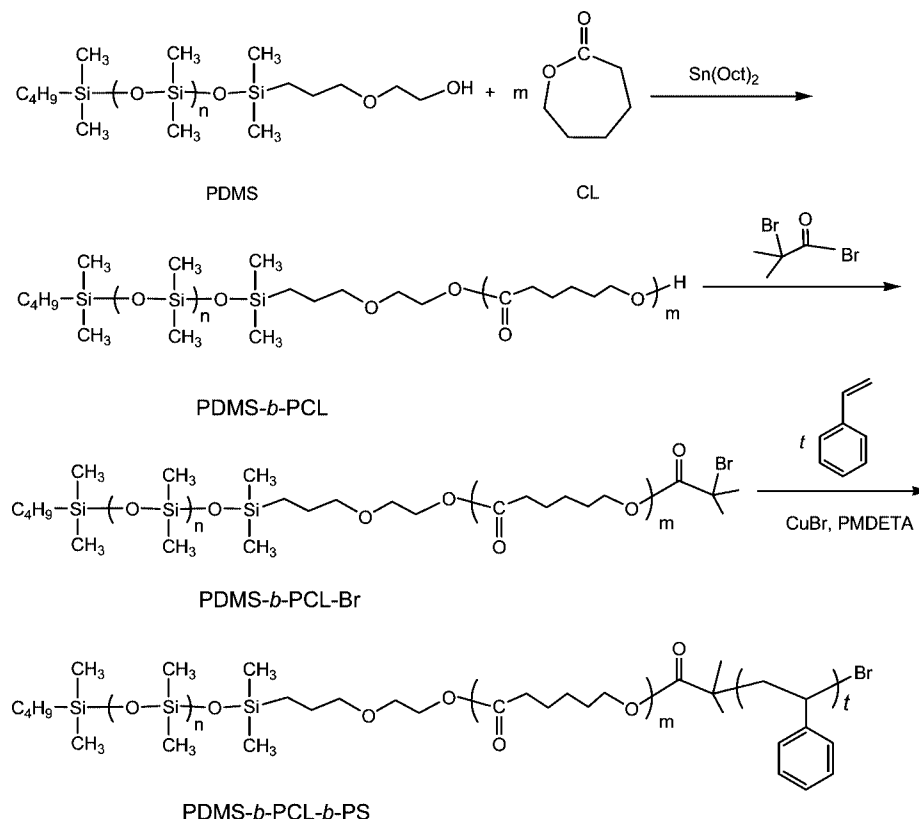
**Measurement and Characterization.** *Nuclear Magnetic Resonance Spectroscopy (NMR).* The block copolymers were dissolved in deuterated chloroform, and the  $^1H$  NMR spectra were measured on a Varian Mercury Plus 400 MHz NMR spectrometer with tetramethylsilane (TMS) as the internal reference.

*Gel Permeation Chromatography (GPC).* The molecular weights of polymers were determined on a Waters 717 Plus autosampler gel permeation chromatography apparatus equipped with Waters RH columns and a Dawn Eos (Wyatt Technology) multiangle laser light scattering detector, and the measurements were carried out at 25 °C with tetrahydrofuran as the eluent at the rate of 1.0 mL/min.

*Atomic Force Microscopy (AFM).* The samples in bulk for AFM observation were trimmed using a microtome machine, and the thickness of the section was about 70 nm. The morphological observation of the samples was conducted on a Nanoscope IIIa scanning probe microscope (Digital Instruments, Santa Barbara, CA) in a tapping mode. A tip fabricated from silicon (125  $\mu$ m in length with ca. 500 kHz resonant frequency) was used for scan. Typical scan speeds during recording were 0.3–1.0 line  $s^{-1}$  using scan heads with a maximum range of 16  $\mu$ m  $\times$  16  $\mu$ m.

*Small-Angle X-ray Scattering (SAXS).* The SAXS measurements were taken on a Bruker Nanostar system. Two-dimensional diffraction patterns were recorded using an image-intensified CCD detector. The experiments were carried out at room temperature (25 °C) using Cu K $\alpha$  radiation ( $\lambda = 1.54$  Å, wavelength) operating at 40 kV, 35 mA. The intensity profiles were output as the plot of scattering intensity ( $I$ ) vs scattering vector,  $q = (4/\lambda) \sin(\theta/2)$  ( $\theta$  = scattering angle).

*Differential Scanning Calorimetry (DSC).* The calorimetric measurements were performed on a Perkin-Elmer Pyris 1 differential scanning calorimeter in a dry nitrogen atmosphere. An

Scheme 1. Synthesis of PDMS-*b*-PCL-*b*-PS Triblock Copolymer

indium standard was used for temperature and enthalpy calibrations. First, all the samples (about 8.0 mg in weight) were heated from  $-70$  to  $180$   $^{\circ}\text{C}$  to record the thermograms of the first DSC scans; the samples held at this temperature for 3 min to remove the thermal history, followed by quenching to  $-70$   $^{\circ}\text{C}$  for the second DSC scans. A heating rate of  $20$   $^{\circ}\text{C}/\text{min}$  was used at all cases. The glass transition temperature ( $T_g$ ) was taken as the midpoint of the heat capacity change. The melting temperatures ( $T_m$ ) were taken as the temperatures of the maximum of endothermic transition.

## Results

**Synthesis of PDMS-*b*-PCL-*b*-PS ABC Triblock Copolymer.** The route of synthesis for PDMS-*b*-PCL-*b*-PS triblock copolymer is summarized in Scheme 1. In the first step, the monocarbinol-terminated polydimethylsiloxane (PDMS-OH) was used to initiate the ring-opening polymerization of  $\epsilon$ -caprolactone with  $\text{Sn}(\text{Oct})_2$  as the catalyst; the hydroxyl-terminated polydimethylsiloxane-*block*-poly( $\epsilon$ -caprolactone) diblock copolymer (PDMS-*b*-PCL-OH) was obtained. The molecular weight of the diblock copolymer was measured by means of gel permeation chromatography (GPC) to be  $M_n = 9300$  with  $M_w/M_n = 1.32$  (see Figure 1). The hydroxyl-terminated PDMS-*b*-PCL diblock copolymer was further employed to react with 2-bromoisobutyryl bromide to afford 2-bromoisobutyryl-terminated PDMS-*b*-PCL diblock copolymer (PDMS-*b*-PCL-Br), which will be used as the macroinitiator for the atom transfer radical polymerization of styrene to obtain the PDMS-*b*-PCL-*b*-PS ABC triblock copolymer. Shown in Figure 2 is the  $^1\text{H}$  NMR spectrum of the resulting product together with the assignment of this spectrum. As indicated in the  $^1\text{H}$  NMR spectrum, the simultaneous appearance of the resonance characteristic of PCL, PDMS, and PS protons indicates that the resulting product combines the structural features of PCL, PDMS, and PS subchains; i.e., the PDMS-*b*-PCL-*b*-PS triblock copolymer was obtained. This polymer was subjected to gel permeation chromatography (GPC) to measure the molecular

weight, and the GPC curve was incorporated in Figure 1. The GPC curve shows that this polymer displayed a unimodal distribution of molecular weight, and the molecular weight was determined to be  $M_n = 25\,600$  with  $M_w/M_n = 1.10$ , indicating that the polymerization was carried out in a living fashion. The results of  $^1\text{H}$  NMR and GPC indicate that the PDMS-*b*-PCL diblock copolymer and PDMS-*b*-PCL-*b*-PS ABC triblock copolymer were successfully obtained.

**Nanostructures of Epoxy Thermosets Containing PDMS-*b*-PCL-*b*-PS.** Before curing, all the mixtures composed of DGEBA, MOCA, and PDMS-*b*-PCL-*b*-PS triblock copolymer are homogeneous and transparent, indicating that no macroscopic phase separation occurred at the scale exceeding the wavelength of visible light. The reactive mixtures were cured at  $150$   $^{\circ}\text{C}$  for 2 h plus  $180$   $^{\circ}\text{C}$  for 2 h to access a complete curing reaction. The thermosets containing the PDMS-*b*-PCL-*b*-PS triblock copolymer up to 40 wt % were prepared. All the thermosets containing the ABC triblock copolymer were homogeneous. When the content of PDMS-*b*-PCL-*b*-PS triblock copolymer is lower than 20 wt %, the thermosetting blends are transparent. When the concentration of PDMS-*b*-PCL-*b*-PS triblock copolymer is 30 wt % or higher, the thermosets became translucent. The epoxy thermosets containing PDMS-*b*-PCL-*b*-PS triblock copolymer were subjected to the morphological investigation by means of atomic force microscopy (AFM) and small-angle X-ray scattering (SAXS).

Shown in Figure 3 are the AFM micrographs of the thermosets containing 10, 20, 30, and 40 wt % PDMS-*b*-PCL-*b*-PS triblock copolymer. The left and right images are the topography and phase contrast images, respectively. It is seen that the microphase-separated morphologies were exhibited in all the cases. For the thermosets containing 10 and 20 wt % PDMS-*b*-PCL-*b*-PS triblock copolymer, the spherical particles were dispersed into continuous matrix (Figures 3A,B). The size of the spherical nanodomains ranged from 50 to 100 nm



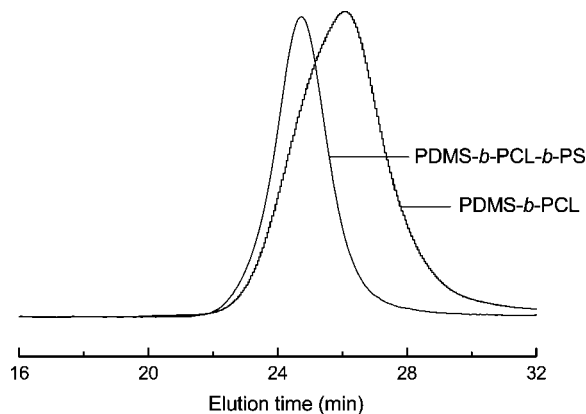


**Figure 1.** GPC curves of PDMS-*b*-PCL diblock and PDMS-*b*-PCL-*b*-PS triblock copolymers.

depending on the content of PDMS-*b*-PCL-*b*-PS triblock copolymer. In terms of the volume fraction of the subchains of the block copolymer and the difference in viscoelastic properties between epoxy matrix and the subchains of triblock copolymer, the dispersed nanodomains are assignable to the immiscible components (i.e., PDMS and PS) whereas the continuous matrix to epoxy, which is miscible with PCL subchain. It is noted that the dispersed nanodomains are not homogeneous and display a “core–shell” structure. In the center of each nanodomain, the “core” is discernible. The “core” could be ascribed to PDMS subchain whereas the “shell” could be attributed to PS subchain. While the content of PDMS-*b*-PCL-*b*-PS triblock copolymer is 30 wt % or more, the thermosets displayed the quite different morphological structures (Figures 3C,D). It is of interest to note that for the thermosets containing 30 wt % PDMS-*b*-PCL-*b*-PS the thermoset shows large-scaled circled and lamellar structures, and all the features are concentric-circled (Figure 3C). The size of each circle is about 20 nm in thickness. To the best of our knowledge, this is the first observation of the formation of concentric-circled nanostructures in epoxy thermosets. It is plausible to propose that the dark domains are responsible for the immiscible subchains (i.e., PDMS and PS) whereas the shallow region is ascribed to epoxy matrix that is miscible with PCL subchains according to the volume fraction of the triblock copolymer. With increasing the content of PDMS-*b*-PCL-*b*-PS triblock copolymer, the concentric-circled lamellar morphology was transformed into the large-scaled lamellar nanostructures (Figure 3D).

The above nanostructured thermosets containing PDMS-*b*-PCL-*b*-PS triblock copolymer were subjected to small-angle X-ray scattering (SAXS) analysis, and the SAXS profiles of the thermosets containing 10, 20, 30, and 40 wt % PDMS-*b*-PCL-*b*-PS triblock copolymer are shown in Figure 4. It is seen that well-defined scattering peaks appear in the scattering curves in all the cases, indicating the formation of the nanostructures in the thermosetting blends. It is noted that the SAXS profiles of the thermosets containing PDMS-*b*-PCL-*b*-PS triblock copolymer of 20 wt % or more exhibited the multiple scattering peaks as denoted with arrows in Figure 4. The appearance of multiple scattering peaks suggests that the long-ranged ordered nanostructures could exist in the thermosets. The intensity of multiple scattering peaks increased with increasing the content of PDMS-*b*-PCL-*b*-PS triblock copolymer, implying that the order of nanostructures is improved. The scattering peaks of the thermosets are situated at the  $q$  values of 1,  $4^{0.5}$ , and  $16^{0.5}$  relative to the first-order scattering peak positions ( $q_m$ ), suggesting that these are lattice scattering peaks of spherical (or cylindrical) nanophases arranged in lamellar lattice. This result is in a good accordance with the observation by means of AFM images.

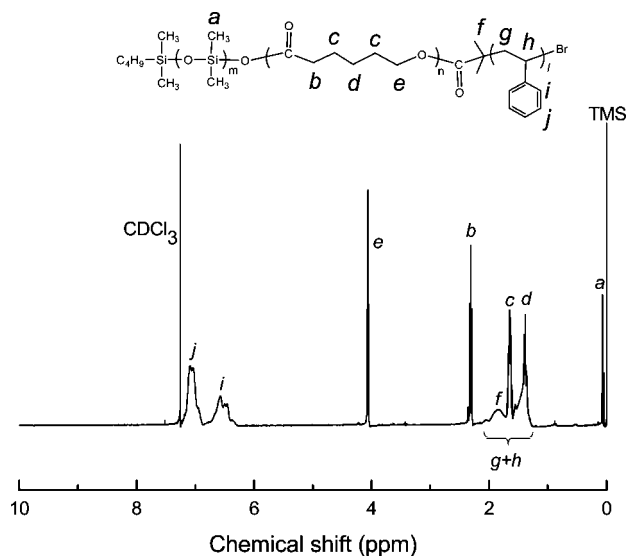


**Figure 2.**  $^1\text{H}$  NMR spectrum of PDMS-*b*-PCL-*b*-PS triblock copolymer.

## Discussion

**Miscibility of Epoxy Blends with Subchains of PMDS-*b*-PCL-*b*-PS.** In order to understand the formation of the above nanostructures, it is critical to know the miscibility and phase behavior of epoxy with the subchains of the ABC triblock copolymer. It has been known that the binary blends of epoxy resin with PCL are miscible after and before curing reaction.<sup>8</sup> Before curing reaction, the miscibility of blends is ascribed to the non-negligible contribution of mixing entropy to free energy of mixing since the molecular weights of precursors of epoxy are quite low. After curing reaction, it has been proved that there are the intermolecular hydrogen-bonding interactions between secondary hydroxyl groups of aromatic amine-cured epoxy and carbonyl groups of PCL after the curing reaction.<sup>8</sup> For the binary blends of epoxy with polystyrene (PS), it was identified that before curing reaction the binary mixtures of DGEBA and PS displayed an upper critical solution temperature (UCST) behavior and the UCST was quite lower than 150 °C (i.e., the curing temperature).<sup>4c,g-i,9</sup> Nonetheless, with the addition of equimolar curing agent (i.e., MOCA) with the respect of DGEBA, the ternary mixtures composed of DGEBA, MOCA, and PS are fully homogeneous; i.e., the UCST behavior no longer displayed due to the alteration of solubility parameter of the system. As for the blends of epoxy with PDMS, it is recognized that the system is immiscible after and before curing reaction owing to the big difference in solubility parameter between epoxy and PDMS.<sup>3c,s,6</sup> In this work, it was observed that the mixtures composed of DGEBA, MOCA, and PDMS were cloudy at room temperature and the elevated temperature (e.g., 150 °C), indicating the immiscibility of epoxy with PDMS after and before curing reaction.

**Nanostructures in Epoxy Thermosets Containing Diblock Copolymers.** In a previous study, we have reported the formation of long-ranged ordered nanostructures in the blends of epoxy thermosets with PS-*b*-PCL diblock copolymer via reaction-induced microphase separation.<sup>4c</sup> Because of the immiscibility of PDMS with epoxy after and before curing reaction, it is expected that the formation of the nanostructures (if any) in the thermosets containing PDMS-*b*-PCL diblock copolymer will follow the mechanism of self-assembly.<sup>3a,b</sup> The morphological structures of epoxy thermosets containing PDMS-*b*-PCL diblock copolymer were examined by means of AFM and SAXS. Shown in Figure 5 are the AFM micrographs of the thermosets containing PDMS-*b*-PCL diblock copolymer. It is

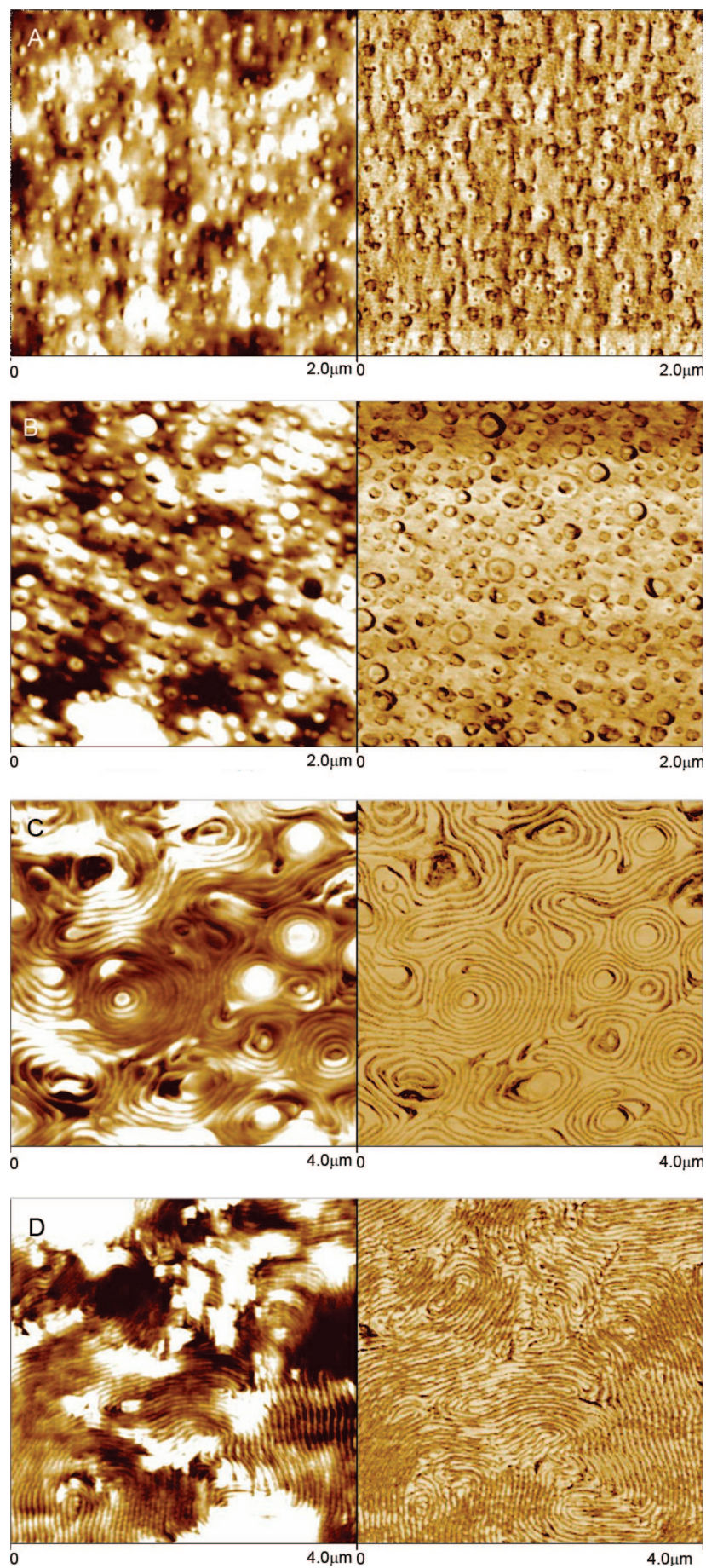


**Figure 3.** AFM images of epoxy thermosets containing PDMS-*b*-PCL-*b*-PS triblock copolymer. Left: height image; Right: phase image. (A) 10, (B) 20, (C) 30, and (D) 40 wt % of PDMS-*b*-PCL-*b*-PS triblock copolymer.



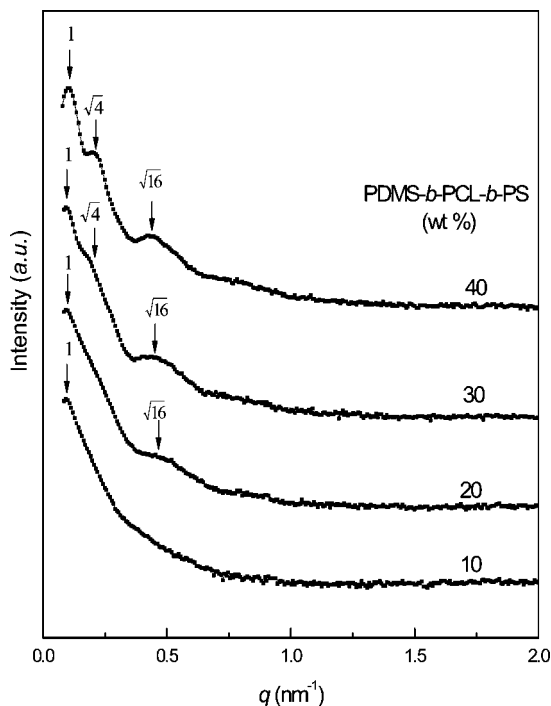


**Figure 4.** SAXS profiles of epoxy thermosets containing PDMS-*b*-PCL-*b*-PS triblock copolymer.

seen that the nanostructures were formed for all the thermosets containing the diblock copolymer. In terms of the volume fraction of PDMS in the thermosetting blend and the difference in viscoelastic properties between the epoxy matrix and PDMS, it is proposed that the spherical nanodomains of 10–20 nm in diameter were ascribed to the subchains of PDMS, which were dispersed in the continuous matrix, whereas the continuous matrix is attributed to the cross-linked epoxy, which are miscible with PCL subchains. The sizes of the spherical PDMS nanodomains almost remain invariant regardless of the composition whereas the distance between the adjacent nanodomains decreased with increasing the content of PDMS-*b*-PCL diblock copolymer. It is noted that the spherical nanodomains become interconnected with increasing the content of diblock copolymer. Some wormlike nanodomains are discernible when the content of diblock copolymer is 30 wt % or more (Figures 5C,D). The morphologies of the thermosets containing PDMS-*b*-PS diblock copolymer were further investigated by small-angle X-ray scattering (SAXS), and the SAXS profiles are shown in Figure 6. For each thermosetting blend, a single scattering peak was displayed in the neighbor of  $q_m = 0.5 \text{ nm}^{-1}$ , indicating that the thermosets containing PDMS-*b*-PCL are microphase-separated. According to the position of the primary scattering peaks the average distance ( $L = 2\pi/q_m$ ) between neighboring PDMS nanodomains can be estimated to be 16.5, 15.3, 13.7, and 12.6 nm for the thermosets containing 10, 20, 30, and 40 wt % PDMS-*b*-PCL diblock copolymer, respectively. The SAXS results are in a good agreement with those obtained by means of AFM. It should be pointed out that the lengths of subchains (i.e., PDMS and PCL) in the model diblock copolymer were identical with those in PDMS-*b*-PCL-*b*-PS triblock copolymer.

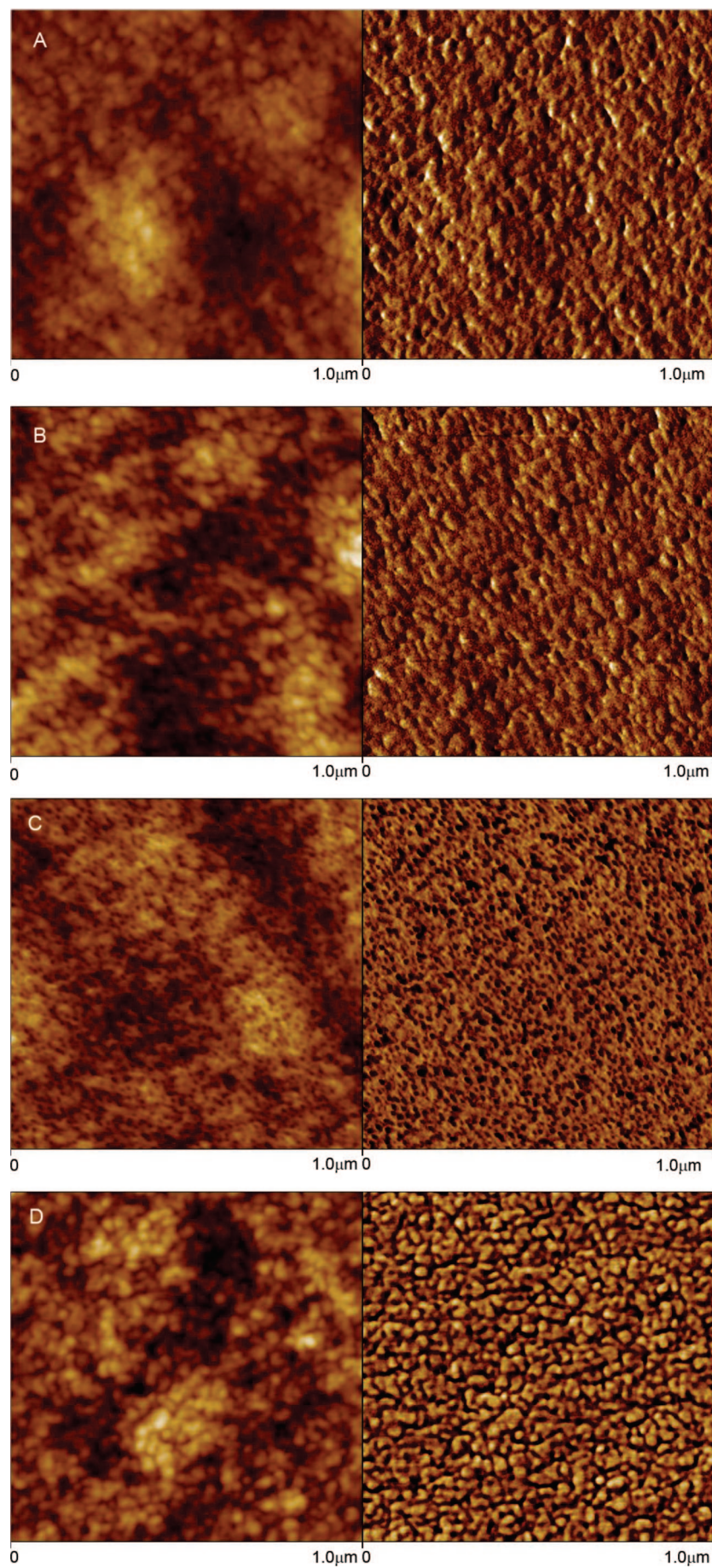
**Reaction-Induced Microphase Separation of PS Blocks in the Presence of PDMS Nanophases.** The utilization of PDMS-*b*-PCL-*b*-PS ABC triblock copolymer to access the nanostructures of epoxy thermosets is based on the following knowledge that (i) the formation of nanostructures in epoxy thermosets containing PDMS-*b*-PCL diblock copolymer would follow the self-assembly mechanism and (ii) the formation of

nanostructures in epoxy thermosets containing PS-*b*-PCL diblock copolymer follow the mechanism of reaction-induced microphase separation (RIMS). Therefore, both self-assembly and RIMS mechanisms would be concurrently involved with the formation of nanostructures in epoxy thermosets containing PDMS-*b*-PCL-*b*-PS triblock copolymer. It is proposed that in the ABC triblock copolymer-containing system the PDMS subchains were first self-organized into spherical or wormlike nanodomains depending on the concentration of the triblock copolymer prior to the curing reaction. The preformed PDMS nanophases could act as the template of the reaction-induced microphase separation of PS subchains and confine the microphase separation of the PS subchains around the PDMS nanophases. When the content of PDMS-*b*-PCL-*b*-PS triblock copolymer is relatively low, the PDMS subchains could be self-organized into separate spherical micelles, and thus the spherical nanophases with so-called “core–shell” structure were displayed in the epoxy thermosets (see Figures 3A,B). With increasing the concentration of PDMS-*b*-PCL-*b*-PS, the self-organized PDMS nanophases became interconnected and wormlike nanoobjects before curing reaction (see Figures 5C,D). The interconnected (or wormlike) PDMS nanophases will template the RIMS of PS subchains into the lamellar structures, and thus the large-scaled lamellar nanostructures were obtained for the thermosets containing 30 and 40 wt % PDMS-*b*-PCL-*b*-PS triblock copolymer. The formation of nanostructures in the epoxy thermosets containing PDMS-*b*-PCL-*b*-PS can be depicted in Scheme 2.

It has been proposed that toughening of thermosets via the formation of nanostructures are quite dependent on type and shape of dispersed microdomains and the mechanisms could involving either the debonding of micelles (or vesicles) from epoxy matrix or crack deflection and frictional interlocking for the thermosets possessing the terraced morphology.<sup>31,u</sup> In the present case, the incorporation of PDMS-*b*-PCL-*b*-PS ABC triblock copolymer facilitates the formation of the “core–shell”, “concentric-circled”, and lamellar nanostructures depending on the composition. It will be of interest to investigate the correlation of the specific nanostructures with the fracture toughness.

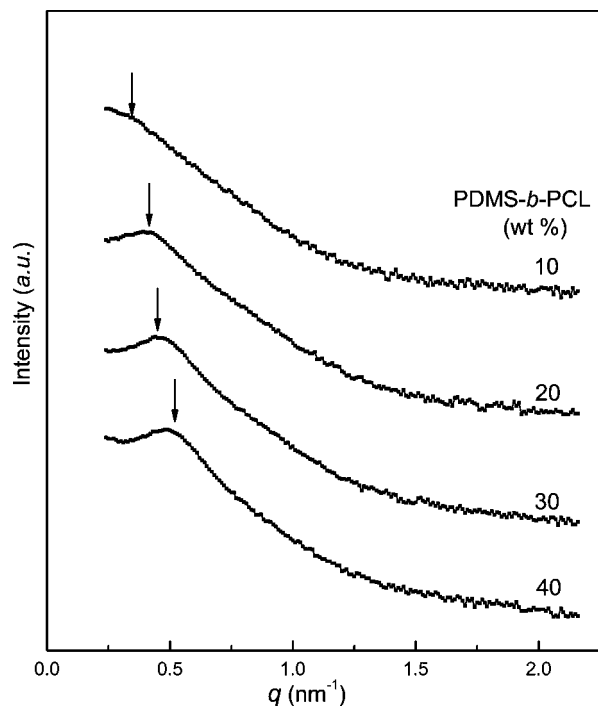
#### Effect of PDMS and PS Nanophases on Mixing of PCL Subchain with Epoxy.

It is proposed that the midblock (i.e., PCL block) of the PDMS-*b*-PCL-*b*-PS ABC triblock copolymer in the thermosetting blends remains miscible with the MOCA-cured epoxy thermosets. The mixing of PCL block with epoxy thermosets was readily evidenced by means of Fourier transform infrared spectroscopy (FTIR). Shown in Figure 7 are the FTIR spectra of the epoxy thermosets containing PDMS-*b*-PCL-*b*-PS triblock copolymer in the range of 1780–1680  $\text{cm}^{-1}$ . For comparison, the FTIR spectrum of PDMS-*b*-PCL-*b*-PS triblock copolymer is also incorporated in this figure. The absorption band in this range is ascribed to the stretching vibration of carbonyl groups. Now that PCL block of PDMS-*b*-PCL-*b*-PS is composed of amorphous and crystalline regions at the room temperature, the infrared curve of the triblock copolymer is comprised of two components at 1725 and 1735  $\text{cm}^{-1}$ , respectively. The component at 1735  $\text{cm}^{-1}$  is assignable to the stretching vibration of carbonyl of PCL in the amorphous region while that at 1725  $\text{cm}^{-1}$  denotes the stretching vibration of carbonyls in the crystalline region of PCL. Upon adding the triblock copolymer into epoxy thermosets, it is seen that the band of stretching vibration assignable to PCL chain in the crystalline region disappeared. This observation implies that the PCL macromolecular chains could be trapped in the thermosets and are no longer crystallizable. In the meantime, the new bands at the lower frequency (i.e., 1712  $\text{cm}^{-1}$ ) appeared. The new shoulder bands are ascribed to the stretching vibration of the carbonyl groups which



**Figure 5.** AFM images of epoxy thermosets containing PDMS-*b*-PCL diblock copolymer. Left: height image; right: phase image. (A) 10, (B) 20, (C) 30, and (D) 40 wt % of PDMS-*b*-PCL diblock copolymer.

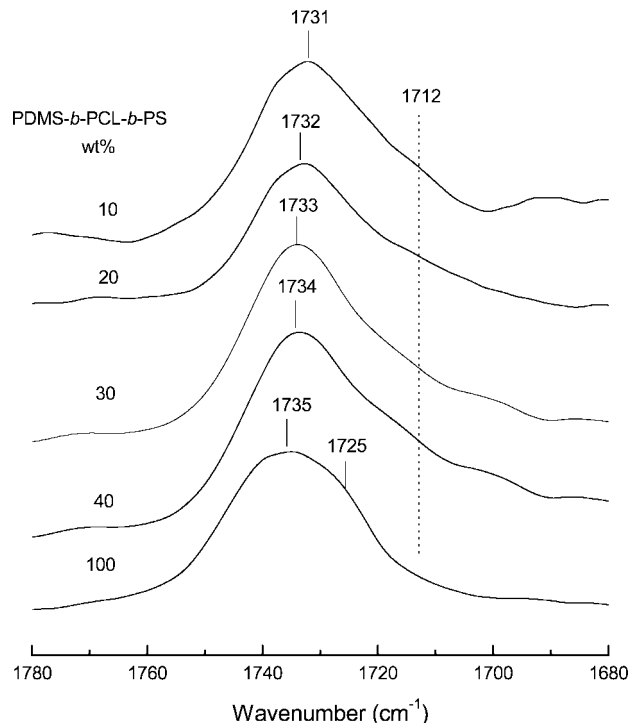




**Figure 6.** SAXS profiles of epoxy thermosets containing PDMS-*b*-PCL diblock copolymer.

are hydrogen-bonded with the secondary hydroxyl groups of MOCA-cured epoxy.<sup>10</sup> In addition, it is noted that the band of carbonyl groups at 1735 cm<sup>-1</sup> was shifted to lower frequency 1731 cm<sup>-1</sup> with increasing the content of epoxy thermoset. The FTIR spectroscopy suggests that the midblock of PDMS-*b*-PCL-*b*-PS triblock copolymer remain miscible with the epoxy thermosets.

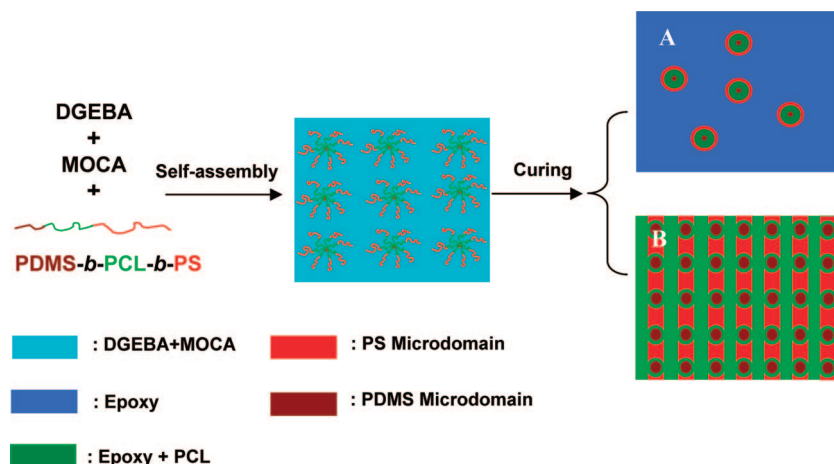
The degree of PCL mixing with epoxy thermosets can be further evaluated by means of differential scanning calorimetry (DSC) in terms of glass transition behavior. Toward this end, the thermosets containing PDMS-*b*-PCL-*b*-PS triblock copolymer were subjected to the thermal analysis. Shown in Figure 8 are DSC curves of the control epoxy, PDMS-*b*-PCL-*b*-PS, and their thermosetting blends. The glass transition temperature ( $T_g$ ) of the control epoxy is about 151 °C. In the DSC curve of PDMS-*b*-PCL-*b*-PS triblock copolymer, a sharp melting transition at ca. 46 °C and a glass transition at ca. 80 °C are displayed. The melting transition is ascribed to the crystalline PCL block whereas the glass transition is responsible for the PS block. The fact that the melting transition of PCL block appeared prior to



**Figure 7.** FTIR spectra of PDMS-*b*-PCL-*b*-PS triblock copolymer and its blends with epoxy thermosets in the range of 1680–1780 cm<sup>-1</sup>.

the glass transition of PS block indicates that the triblock copolymer is microphase-separated. It should be pointed out that the  $T_g$  of PDMS domain (ca. -123 °C) is beyond the range of the experimental temperature (-70 to 200 °C). It is noted that all the thermosets investigated did not exhibit the melting transition of PCL block, suggesting that the PCL block are not crystalline in the nanostructured thermosets. It is proposed that the PCL blocks were interpenetrated in the cross-linked epoxy networks; i.e., the PCL block are miscible with the epoxy networks. This result is in a good agreement with the FTIR spectroscopy in view of the disappearance of the stretching vibration bands of PCL crystals (see Figure 7). The miscibility was further evidenced by the depression in glass transition temperatures ( $T_g$ 's) for the epoxy-rich phases as shown in Figure 8. It is seen that each thermosetting blend containing the diblock copolymers displayed single  $T_g$ , which was decreased with increasing the concentration of the triblock copolymers. The decreased  $T_g$ 's resulted from the plasticization of miscible PCL on epoxy matrix. It should be pointed out that the indicated

**Scheme 2.** Formation of Nanostructures in Epoxy Thermosets Containing PDMS-*b*-PCL-*b*-PS ABC Triblock Copolymer





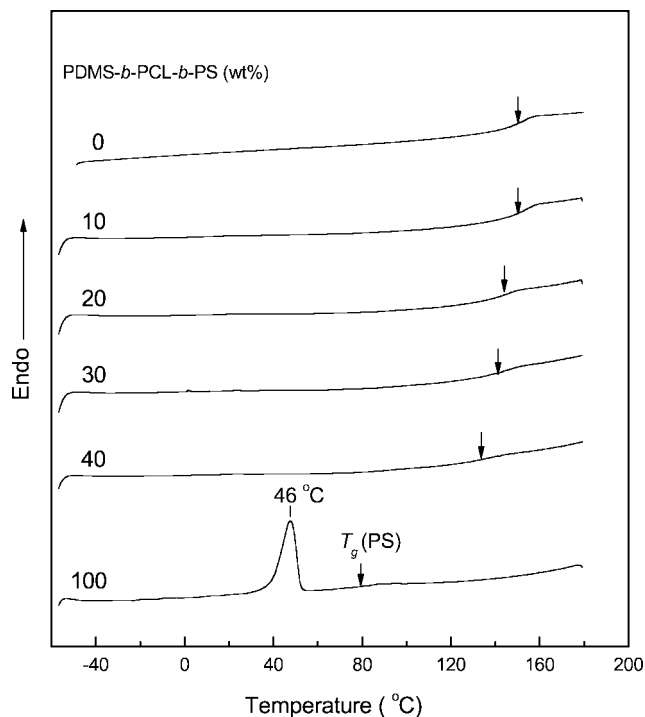


**Figure 8.** DSC curves of the nanostructured epoxy thermostets containing PDMS-*b*-PCL diblock copolymer.

$T_g$ 's in Figure 8 are only ascribed to the epoxy matrix that is miscible with PCL block since the glass transition temperatures of the microphase-separated PS domains are much lower than the values of the  $T_g$ 's. In addition, the  $T_g$  of the PDMS nanophases ( $\sim 123$  °C) is beyond the temperature range of the present DSC measurement. The  $T_g$  value of the epoxy matrix can be employed to evaluate the mixing status of the PCL block with epoxy thermostets.

There are several theoretical and empirical equations to account for the dependence of  $T_g$  on composition in miscible polymer blends.<sup>11</sup> Of them, the Couchman equation<sup>11c</sup> is frequently used:

$$\ln T_g = [W_1 k \ln T_{g1} + W_2 \ln T_{g2}] / (W_1 k + W_2) \quad (1)$$

where  $W_i$  is the weight fraction of component  $i$  and  $T_g$  is the glass transition temperature of blend; the parameter  $k$  is Couchman coefficient defined by

$$k = \Delta C_{p1} / \Delta C_{p2} \quad (2)$$

where  $\Delta C_{pi}$  designates the increment of the heat capacity of the specimen at glass transition. For the binary thermosetting blends of epoxy thermostet with the PCL having the identical molecular weight with the length of PCL block in the block copolymers, the value of  $k$  was determined to be 1.42 (the DSC curves not shown here for brevity) (see Figure 9). Under the identical condition, the thermal analyses were also carried out for the nanostructured epoxy thermostets containing PDMS-*b*-PCL diblock copolymers and the plots of  $T_g$ 's as functions of the concentration of PCL for the nanostructured thermostets are also incorporated in Figure 9. It is noted that the curves of the  $T_g$  versus content of PCL for the nanostructured thermostets containing PDMS-*b*-PCL and PDMS-*b*-PCL-*b*-PS block copolymers was all above that of the thermosetting blends containing the model PCL. Furthermore, the  $T_g$ -composition curve of the thermostets containing the ABC triblock copolymer is above that of those containing PDMS-*b*-PCL diblock copolymer. This observation suggests that with the identical

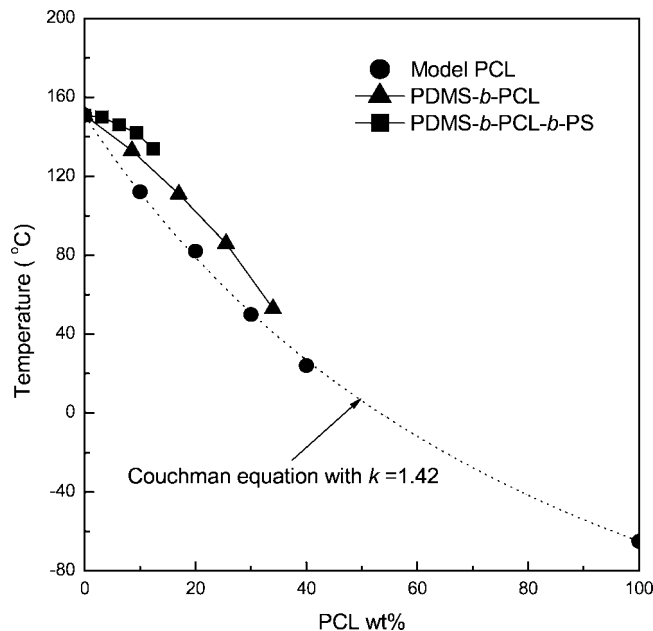


**Figure 9.** Plots of  $T_g$ 's as functions of concentration of PCL for epoxy thermostets containing the block copolymers.

content of PCL block the nanostructured thermostets displayed higher  $T_g$  of epoxy matrix than the binary blends of epoxy with the model PCL and the nanostructured thermostets containing PDMS-*b*-PCL-*b*-PS possess the higher  $T_g$  of epoxy matrix than the nanostructured thermostets containing PDMS-*b*-PCL. It is proposed that for the thermostets containing the diblock (or triblock) copolymer the increased  $T_g$ 's could be associated with the formation of the nanostructures in the thermostets. In the binary thermosetting blends, the PCL chains were homogeneously dispersed into the epoxy matrix and were well interpenetrated into the cross-linked epoxy networks via the formation of the intermolecular hydrogen-bonding interactions. In contrast, the PCL chains have to be enriched at the surfaces of the microphase-separated PDMS nanodomains due to the presence of chemical bonds between PDMS and PCL subchains in the composites. Because of the steric hindrance, the PCL chains at the intimate surface of PS nanodomains could not be well mixed with epoxy matrix, and thus the less PCL chains were interpenetrated with the epoxy matrix in the nanocomposites; i.e., the plasticization of PCL chains on the epoxy matrix would be effectively weakened, which causes the increased  $T_g$ 's of epoxy matrix. This effect has been reported in the self-assembly of epoxy resin and amphiphilic block copolymer nanocomposites.<sup>3a,b</sup> Nonetheless, this effect is increasingly pronounced in the thermostets containing PDMS-*b*-PCL-*b*-PS ABC triblock copolymer due to the presence of two immiscible blocks (i.e., PDMS and PS). In this case, the PCL chains have to be enriched not only at the surfaces of PDMS but also at PS nanodomains since the midblock (viz. PCL) is simultaneously connected with PDMS and PS blocks in the composites. Therefore, there were more demixed PCL chains around the microphase-separated domains, and thus the less PCL chains were interpenetrated with the epoxy matrix in the nanocomposites. The phenomenon that miscible blocks were expelled from the epoxy matrix has been also found in the nanostructured thermostets of epoxy and polystyrene-*block*-polybutadiene-*block*-poly(methyl methacrylate) ABC triblock copolymers.<sup>3g,h</sup>

## Conclusions

The PDMS-*b*-PCL-*b*-PS ABC triblock copolymer was successfully synthesized via the sequential ring-opening polymer-

ization and atom transfer radical polymerization. The block copolymer was incorporated into epoxy to access the nanostructured thermosets. By means of atomic force microscopy and small-angle X-ray scattering, the morphological structures of the thermosets were examined. In view of the difference in miscibility of epoxy with the individual subchain of the triblock copolymers after and before curing reaction, it is proposed that the formation of the nanostructures follows the combined mechanisms of self-assembly and reaction-induced microphase separation. The self-organized nanophases were formed before the curing reaction since the PDMS subchains of the triblock polymer are immiscible with epoxy before curing reaction. With the occurrence of the curing reaction, the PS subchains were gradually microphase-separated out in the presence of the nanophases of PDMS. It is identified that the thermosets can display either core-shell or lamellar nanostructures, quite depending on the concentration of triblock copolymers.

**Acknowledgment.** The financial support from Natural Science Foundation of China (No. 20474038 and 50873059) and National Basic Research Program of China (No. 2009CB930400) is acknowledged. The authors thank Shanghai Leading Academic Discipline Project (Project No. B202) for partial support.

## References and Notes

- (1) Pascault, J. P.; Williams, R. J. J. In *Polymer Blends*; Paul, D. R., Bucknall, C. B., Eds.; Wiley: New York, 2000; Vol. 1, pp 379–415.
- (2) (a) de Gennes, P.-G. *Scale Concepts in Polymer Physics*; Cornell University Press: Ithaca, NY, 1979. (b) de Gennes, P.-G. *Phys. Lett.* **1969**, *28A*, 725. (c) Ruiz-Pérez, L.; Royston, G. J.; Fairclough, J. A.; Ryan, A. J. *Polymer* **2008**, *49*, 4475.
- (3) (a) Hillmyer, M. A.; Lipic, P. M.; Hajduk, D. A.; Almdal, K.; Bates, F. S. *J. Am. Chem. Soc.* **1997**, *119*, 2749. (b) Lipic, P. M.; Bates, F. S.; Hillmyer, M. A. *J. Am. Chem. Soc.* **1998**, *120*, 8963. (c) Mijovic, J.; Shen, M.; Sy, J. W.; Mondragon, I. *Macromolecules* **2000**, *33*, 5235. (d) Grubbs, R. B.; Dean, J. M.; Broz, M. E.; Bates, F. S. *Macromolecules* **2000**, *33*, 9522. (e) Kosonen, H.; Ruokolainen, J.; Nyholm, P.; Ikkala, O. *Macromolecules* **2001**, *34*, 3046. (f) Guo, Q.; Thomann, R.; Gronski, W. *Macromolecules* **2002**, *35*, 3133. (g) Ritzenthaler, S.; Court, F.; Girard-Reydet, E.; Leibler, L.; Pascault, J. P. *Macromolecules* **2002**, *35*, 6245. (h) Ritzenthaler, S.; Court, F.; Girard-Reydet, E.; Leibler, L.; Pascault, J. P. *Macromolecules* **2003**, *36*, 118. (i) Rebizant, V.; Abetz, V.; Tournilhac, T.; Court, F.; Leibler, L. *Macromolecules* **2003**, *36*, 9889. (j) Dean, J. M.; Verghese, N. E.; Pham, H. Q.; Bates, F. S. *Macromolecules* **2003**, *36*, 9267. (k) Rebizant, V.; Venet, A. S.; Tournilhac, F.; Girard-Reydet, E.; Navarro, C.; Pascault, J. P.; Leibler, L. *Macromolecules* **2004**, *37*, 8017. (l) Dean, J. M.; Grubbs, R. B.; Saad, W.; Cook, R. F.; Bates, F. S. *J. Polym. Sci., Part B: Polym. Phys.* **2003**, *41*, 2444. (m) Wu, J.; Thio, Y. S.; Bates, F. S. *J. Polym. Sci., Part B: Polym. Phys.* **2005**, *43*, 1950. (n) Zucchi, I. A.; Galante, M. J.; Williams, R. J. J. *Polymer* **2005**, *46*, 2603. (o) Thio, Y. S.; Wu, J.; Bates, F. S. *Macromolecules* **2006**, *39*, 7187. (p) Serrano, E.; Tercjak, A.; Kortaberria, G.; Pomposo, J. A.; Mecerreyes, D.; Zafeiropoulos, N. E.; Stamm, M.; Mondragon, I. *Macromolecules* **2006**, *39*, 2254. (q) Ocando, C.; Serrano, E.; Tercjak, A.; Peña, C.; Kortaberria, G.; Calberg, C.; Grignard, B.; Jerome, R.; Carrasco, P. M.; Mecerreyes, D.; Mondragon, I. *Macromolecules* **2007**, *40*, 4086. (r) Maiez-Tribut, S.; Pascault, J. P.; Soule, E. R.; Borrajo, J.; Williams, R. J. J. *Macromolecules* **2007**, *40*, 1268. (s) Gong, W.; Zeng, K.; Wang, L.; Zheng, S. *Polymer* **2008**, *49*, 3318. (t) Wu, J.; Thio, Y. S.; Bates, F. S. *J. Polym. Sci., Part B: Polym. Phys.* **2005**, *43*, 1950. (u) Dean, J. M.; Lipic, P. M.; Grubbs, R. B.; Cook, R. F.; Bates, F. F. *J. Polym. Sci., Part B: Polym. Phys.* **2001**, *39*, 2996.
- (4) (a) Meng, F.; Zheng, S.; Zhang, W.; Li, H.; Liang, Q. *Macromolecules* **2006**, *39*, 711. (b) Serrano, E.; Tercjak, A.; Kortaberria, G.; Pomposo, J. A.; Mecerreyes, D.; Zafeiropoulos, N. E.; Stamm, M.; Mondragon, I. *Macromolecules* **2006**, *39*, 2254. (c) Meng, F.; Zheng, S.; Li, H.; Liang, Q.; Liu, T. *Macromolecules* **2006**, *39*, 5072. (d) Meng, F.; Zheng, S.; Liu, T. *Polymer* **2006**, *47*, 7590. (e) Sinturel, C.; Vayer, M.; Erre, R.; Amenitsch, H. *Macromolecules* **2007**, *40*, 2532. (f) Ocando, C.; Serrano, E.; Tercjak, A.; Pena, C.; Kortaberria, G.; Calberg, C.; Grignard, B.; Jerome, R.; Carrasco, P. M.; Mecerreyes, D.; Mondragon, I. *Macromolecules* **2007**, *40*, 4068. (g) Xu, Z.; Zheng, S. *Macromolecules* **2007**, *40*, 2548. (h) Meng, F.; Xu, Z.; Zheng, S. *Macromolecules* **2008**, *41*, 1411. (i) Fan, W.; Zheng, S. *Polymer* **2008**, *49*, 3157.
- (5) Flory, P. J. *Principles of Polymer Chemistry*; Cornell University Press: Ithaca, NY, 1953.
- (6) (a) Takahashi, T.; Nakajima, N.; Saito, N. In *Rubber-Toughened Plastics*; Adv. Chem. Ser. 222; Riew, C. K., Ed.; American Chemical Society: Washington, DC, 1989. (b) Buchholz, U.; Mülhaupt, R. *Polym. Prepr.* **1992**, *33*, 205. (c) Könczöl, L.; Döll, W.; Buchholz, U.; Mülhaupt, R. *J. Appl. Polym. Sci.* **1994**, *54*, 815. (d) Guo, Q.; Chen, F.; Wang, K.; Chen, L. *J. Polym. Sci., Part B: Polym. Phys.* **2006**, *44*, 3042. (e) Xu, Z.; Zheng, S. *Polymer* **2007**, *48*, 6134.
- (7) Wang, J. S.; Matyjaszewski, K. *J. Am. Chem. Soc.* **1995**, *117*, 5614.
- (8) (a) Yin, M.; Zheng, S. *Macromol. Chem. Phys.* **2005**, *206*, 929. (b) Ni, Y.; Zheng, S. *Polymer* **2005**, *46*, 5828.
- (9) (a) Hoppe, C. E.; Galante, M. J.; Oyanguren, P. A.; Williams, R. J. J.; Girard-Reydet, E.; Pascault, J. T. *Polym. Eng. Sci.* **2002**, *42*, 2361. (b) Zucchi, I. A.; Galante, M. J.; Borrajo, J.; Williams, R. J. J. *Macromol. Chem. Phys.* **2004**, *205*, 676.
- (10) (a) Coleman, M. M.; Painter, P. C. *Prog. Polym. Sci.* **1995**, *20*, 1. (b) Coleman, M. M.; Graf, J. F.; Painter, P. C. *Specific Interactions and the Miscibility of Polymer Blends*; Technomic Publishing: Lancaster, PA, 1991. (c) Hu, Y.; Motze, H. R.; Etxeberria, A. M.; Fernandez-Berridi, H. J.; Iruin, J. J.; Painter, P. C.; Coleman, M. M. *Macromol. Chem. Phys.* **2000**, *201*, 705. (d) Coleman, M. M.; Moskala, E. J. *Polymer* **1983**, *24*, 251.
- (11) (a) Fox, T. G. *Bull. Am. Phys. Soc.* **1956**, *1*, 123. (b) Gordon, M.; Taylor, J. S. *J. Appl. Chem.* **1952**, *2*, 496. (c) Couchman, P. R. *Macromolecules* **1978**, *11*, 1156.

MA8018014